Plasma and Thermal ALD of Al_2O_3 in a Commercial 200 mm ALD Reactor

J. L. van Hemmen, S. B. S. Heil, J. H. Klootwijk, F. Roozeboom, C. J. Hodson, M. C. M. van de Sanden and W. M. M. Kessels

J. Electrochem. Soc. 2007, Volume 154, Issue 7, Pages G165-G169.
doi: 10.1149/1.2737629

Journal of The Electrochemical Society, **154** (7) G165-G169 (2007)
0013-4651/2007/154(7)/G165/5/$20.00 © The Electrochemical Society

Plasma and Thermal ALD of Al_2O_3 in a Commercial 200 mm ALD Reactor

J. L. van Hemmen,[a] S. B. S. Heil,[a,*] J. H. Klootwijk,[b] F. Roozeboom,[c,] C. J. Hodson,[d] M. C. M. van de Sanden,[a] and W. M. M. Kessels[a,**,z]**

[a]*Department of Applied Physics, Eindhoven University of Technology, 5600 MB Eindhoven, The Netherlands*
[b]*Philips Research Laboratories, 5656 AE Eindhoven, The Netherlands*
[c]*NXP Semiconductors Research, 5656 AE Eindhoven, The Netherlands*
[d]*Oxford Instruments Plasma Technology, North End, Yatton BS49 4AP, United Kingdom*

The deposition of Al_2O_3 by remote plasma atomic layer deposition (ALD) in the Oxford Instruments FlexAL reactor was studied and compared with results from thermal ALD in the same reactor. Trimethylaluminum [$Al(CH_3)_3$] was used as the metal precursor and O_2 plasma and H_2O were used as oxidizing agents for the plasma and thermal processes, respectively. For remote plasma ALD with a total cycle time of 4 s, the growth per cycle decreased monotonically with substrate temperature, from 1.7 Å/cycle at 25°C to 1.0 Å/cycle at 300°C. This growth per cycle was consistently higher than that obtained for thermal ALD. For the latter a maximum growth per cycle of ~1.0 Å/cycle was found at 200°C. The film properties investigated were nearly independent of oxidant source for temperatures between 100 and 300°C, with a slightly higher mass density for the remote plasma ALD Al_2O_3 films. Films deposited at 200 and 300°C were stoichiometric with a mass density of 3.0 g/cm^3 and low C (<1 atom %) and H (<3 atom %) contents. At lower substrate temperatures, oxygen-rich films were obtained with a lower mass density and higher H-content. Remote plasma ALD produced uniform Al_2O_3 films with nonuniformities of less than ±2% over 200 mm diam substrates. Excellent conformality was obtained for films deposited in macropores with an aspect ratio of ~8 (2.0–2.5 μm diam). Preliminary results on electrical properties of remote plasma deposited films showed high dielectric constants of 7.8 and 8.9 for as-deposited and forming gas annealed Al_2O_3, respectively.
 [DOI: 10.1149/1.2737629]

Manuscript submitted February 2, 2007; revised manuscript received March 5, 2007. Available electronically May 21, 2007.

Al_2O_3 is of interest for a wide range of applications because of its unique material properties. The most commonly investigated application is as a dielectric layer, for example as a gate oxide in complementary metal oxide semiconductor (CMOS)[1,2] or as a capacitor dielectric in dynamic random access memory (DRAM).[3] Al_2O_3 is considered for these applications as it combines a high dielectric constant ($k \sim 9$) with a high band gap (~9 eV). These properties make Al_2O_3 an interesting material as a dielectric in high density trench capacitors, e.g., for radio-frequency (rf) decoupling capacitors integrated in silicon.[4-6] Additionally, Al_2O_3 attracts interest in emerging technologies involving organic electrical devices and photovoltaics, e.g., as transparent, high-density moisture permeation barrier for organic light emitting devices (OLEDs)[7-9] and as a surface passivation layer on high-efficiency crystalline silicon solar cells.[10] Furthermore, Al_2O_3 has excellent mechanical properties and can be used as a wear resistive coating on, for example, microelectromechanical systems (MEMS).[11]

Critical for all these applications is to have a deposition technique that is capable of producing high-quality films with low pinhole density and good conformality on substrates with demanding topologies, and which offers precise thickness control even over large-area substrates. Atomic layer deposition (ALD) of Al_2O_3 is a method that has shown great potential to meet these demands. This chemical vapor deposition (CVD) method is cyclic and based on two separately executed half reactions that are self-limiting: (*i*) chemisorption of the metal precursor and (*ii*) oxidation of the metal and removal of the organic surface groups. Thermal ALD of amorphous Al_2O_3 using trimethylaluminum [$Al(CH_3)_3$] as the metal precursor and H_2O as the oxidant has already been widely investigated and can be considered as a model system for ALD.[12] In this process, $Al(CH_3)_3$ chemisorbs to surface hydroxyl groups by splitting off gaseous CH_4. After reaching saturation, residual $Al(CH_3)_3$ and reaction products are removed by purging and/or pumping. Subsequently, the $-CH_3$ ligands of the chemisorbed $Al(CH_3)_3$ species are removed by a reaction with H_2O leading to an additional submonolayer of Al_2O_3 while also regenerating the surface –OH groups.

To widen the ALD process window, O_2 plasmas[2,7-10,13-18] and O_3[13,14,19] have recently been considered as alternative oxidants. Particularly O_2 plasmas are very effective oxidants that can easily remove organic ligands by O-radical driven combustion-like surface reactions.[18] Therefore, the plasma-based process generally yields more process flexibility,[20] including the potential of depositing higher quality materials at lower substrate temperatures while also avoiding the use of the difficult-to-purge H_2O. The plasma assisted processes can be divided in three categories: (*i*) direct plasma ALD where the substrates are positioned on an electrode used for plasma creation,[2,7,13,15,16,21] (*ii*) remote plasma ALD, where plasma creation takes place remotely from the substrate but with all plasma species still present at the position of the substrate,[8,10,14,18] and (*iii*) radical-enhanced ALD where the plasma is created far from the substrate such that ions and electrons from the plasma do not reach the substrate at all.[17] For direct plasma ALD plasma damage can occur due to high ion energies,[15,22] while for radical-enhanced ALD ion damage is completely absent at the cost of a lower reactivity due to reduced fluxes of reactive species. Remote plasma ALD combines a high reactivity with a low ion energy, typically below the threshold energy for plasma damage.

To date, the studies of plasma-assisted ALD of Al_2O_3 employed mostly direct plasma ALD reactors with the main focus the electrical properties of the material as well as the properties of the interface with the Si substrate (e.g., interfacial oxide formation). These aspects were also addressed in a comparison between remote plasma and thermal ALD by Choi et al.[14] The growth characteristics and material properties obtained by radical enhanced ALD of Al_2O_3 were recently studied by Niskanen et al.[17] In this paper, we report on the growth characteristics and material properties of remote plasma ALD Al_2O_3 while also making a comparison with the thermal ALD process of Al_2O_3. Both the remote plasma and thermal process were carried out in the new Oxford Instruments FlexAL ALD tool.[23] The growth per cycle, material atomic composition, and uniformity are reported for a wide substrate temperature range while the conformality and the electrical properties of the Al_2O_3 are also addressed.

Experimental

ALD reactor and film synthesis.— Both the remote plasma and thermal ALD of Al_2O_3 was carried out in the FlexAL ALD tool recently developed by Oxford Instruments Plasma Technology. The

* Electrochemical Society Student Member.
** Electrochemical Society Active Member.
z E-mail: W.M.M.Kessels@tue.nl

system, described extensively in Ref. 23, is an advanced research and development reactor equipped with a loadlock and capable of handling wafers up to 200 mm in diam. For remote plasma ALD the system is equipped with an inductively coupled plasma source located above the wafer. It can be isolated from the reactor by a gate valve. The plasma source can be operated with various gases or gas mixtures. Multiple precursor pods can be connected to the reactor such that several precursors are available simultaneously. The temperature of the precursor pods, the precursor lines, reactor walls, and substrate holder can be individually controlled. Furthermore, the system is equipped with optical viewports that can be used for in situ monitoring of film growth. Especially the techniques of in situ spectroscopic ellipsometry (SE) have proven to be particularly powerful to study ALD processes and the material properties obtained.[24,25]

For Al_2O_3 ALD, trimethylaluminum [TMA,$Al(CH_3)_3$] (Akzo-Nobel, SSG grade) was vaporized at 25°C and a saturated dose was obtained by 20 ms vapor injection using fast switching ALD valves. For the plasma process, the oxidation step took place via a 400 W O_2 plasma at a pressure of 15 mTorr and ignited for a duration of typically 2 s. O_2 also served as a purge gas because O_2 does not react with $Al(CH_3)_3$;[18] the O_2 flow was kept constant at 60 sccm during the entire cycle. A cycle time of 4 s was obtained by employing an $Al(CH_3)_3$ purge of 1.5 s and a post-plasma-purge of 0.5 s.For thermal ALD, H_2O was vaporized at 25°C and dosed in steps of at maximum 120 ms. If higher doses were required the 120 ms step was repeated with 0.5 s intermediate delays. A 110 sccm Ar flow at a pressure of 15 mTorr was used as purge gas and a pump-purge step (7 s evacuation and 5 s purging) was found most effective in removing residual H_2O from the reactor. Typical cycle times for the thermal ALD process were 16 s but it should be noted that no efforts were undertaken to optimize this cycle time. This can for example be done by increasing the residence time during water exposure and operating at higher pressure. The substrate temperature was varied between 25 and 300°C for remote plasma ALD. The lowest substrate temperature used for the thermal ALD process was 100°C to avoid extensive purge times necessary to remove H_2O at low temperatures.[26] The reactor wall temperature was kept constant at 120°C, except for the remote plasma depositions at 25°C for which the wall was also kept at 25°C.

Film analysis and characterization.— Si p-type wafers with diameters up to 200 mm were used as substrates for characterization of the ALD process and film composition. The center thickness and refractive index of the Al_2O_3 films were monitored in situ by spectroscopic ellipsometry (SE) measurements (J.A. Woollam M-2000D, 193–1000 nm wavelength range) carried out between the ALD cycles. Ex situ measurements with the same ellipsometer were performed to measure the film thickness on any position of the wafer to obtain the nonuniformity of the films as defined by

$$\text{nonuniformity} = \frac{d_{\max} - d_{\min}}{2d_{\text{average}}} \quad [1]$$

where $d_{\max}$, $d_{\min}$, and d_{average} are the maximum, minimum, and average thickness, respectively. The Al, O, and C-content of the film were determined by Rutherford backscattering spectrometry (RBS). Elastic recoil detection (ERD) was used to determine the H-content. A 2 MeV $^4He^+$ beam was applied in these measurements. The conformality of the remote plasma ALD process was examined for an 80 nm thick Al_2O_3 film deposited in 2–2.5 μm wide and ~19 μm deep silicon macropore structures. After sputtering a 2 nm platinum conductive layer for imaging purposes, high-resolution scanning electron microscopy (SEM) images using a FEI Nova NanoSEM 600 electron microscope revealed the conformality. For electrical characterization of the Al_2O_3 films, the Si substrates were HF-dipped (1% HF solution) prior to deposition to remove the native oxide. Aluminum electrodes (areas ranging from 0.02 to 1.2 mm^2) were sputtered on the Al_2O_3 films using a shadow mask.

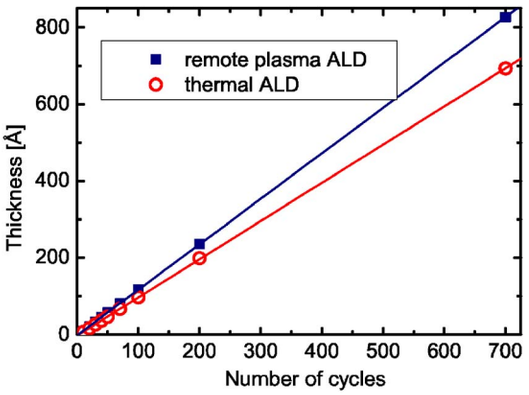

Figure 1. (Color online) Al_2O_3 film thickness as a function of the number of cycles for both remote plasma ALD and thermal ALD. The thickness was determined by in situ spectroscopic ellipsometry and the growth per cycle was obtained from the linear fits shown in the figure. The substrate temperature was 200°C.

Both as-deposited and forming gas annealed films (30 min 425°C, 10% H_2-90% N_2) were characterized electrically. The dielectric constant and breakdown voltage of these test structures were determined by 10 kHz capacitance-voltage (C-V) and current-voltage (I-V) measurements with an HP4275A multifrequency LCR meter and an Agilent 4155B parameter analyzer.

Results and Discussion

Growth per cycle and saturation behavior.— Figure 1 shows an in situ SE measurement of the Al_2O_3 film thickness as a function of the completed number of ALD cycles for both the remote plasma and the thermal ALD process. The substrate temperature was 200°C. As expected, the thickness increases linearly with the number of completed ALD cycles for both the remote plasma and the thermal ALD process. From these in situ thickness measurements the growth per cycle (GPC) can be determined from a linear fit of the data. Clearly, the growth per cycle is higher for remote plasma ALD than for thermal ALD, i.e., 1.2 Å/cycle for remote plasma ALD and 1.0 Å/cycle for thermal ALD.

The saturation behavior of the oxidation step was investigated for the remote plasma and thermal ALD by considering the GPC as a function of the O_2 plasma exposure time and H_2O dosing time. For remote plasma ALD, the results are shown in Fig. 2 for a substrate temperature of 200°C. The corresponding nonuniformity of the film thickness over a 150 mm wafer is also given. Figure 2 reveals that surface reactions saturate during the oxidation step when the O_2 plasma exposure time is greater than 1.0 s, with a saturated value of the GPC of 1.2 Å/cycle. For shorter plasma exposure times, the GPC is not saturated and the plasma step becomes a source of film nonuniformity. This can be explained by a shortage of oxidizing plasma species at these short plasma exposure times. In this subsaturated regime the growth rate is slightly higher in the center where the flux of plasma species is greatest. Note that if the surface reaction kinetics were slow, the flux of plasma species would be more isotropic within the reactor and a good uniformity would also be achieved at plasma exposure times shorter than required for saturation. For a plasma exposure of 2 s the growth per cycle was found to saturate over the whole substrate area for all substrate temperatures investigated between 25 and 300°C. The nonuniformity determined over 200 mm wafers decreased from 1.2% at 25°C to 0.5% at 300°C for this setting.

Figure 3 shows the GPC for the thermal process as a function of H_2O dosing time for substrate temperatures of 100 and 200°C. Different pump and purge steps have been used for the different data points shown in Fig. 3, which can explain the scatter between data points. Note that the H_2O dosing time required to obtain saturation

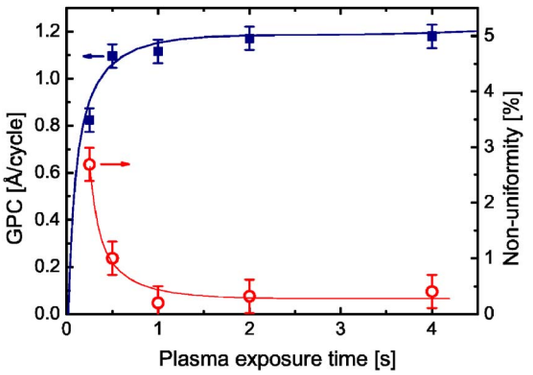

Figure 2. (Color online) The growth per cycle (GPC) and nonuniformity for remote plasma ALD Al_2O_3 as a function of plasma exposure time. The nonuniformity was determined over a 150 mm wafer. The substrate temperature was 200°C and a 400 W plasma power was used. The lines serve as a guide to the eye.

is significantly longer than the $Al(CH_3)_3$ dosing time of 20 ms, even though the delivery details and vapor pressure are similar for both H_2O and $Al(CH_3)_3$ [saturated vapor pressure of H_2O and $Al(CH_3)_3$ are ~24 and ~16 Torr at 25°C, respectively]. The relatively long time required to achieve saturation of the surface reactions is probably due to slow kinetics of the H_2O half reaction,[27] which also explains the excellent uniformity of the thermal ALD process under all conditions studied. The nonuniformities were <1% as determined over 200 mm wafers. In addition, for shorter cycle times with reduced purging (and pumping) using high H_2O dosing times (>240 ms), a slightly decreased GPC was observed using the same $Al(CH_3)_3$ dose. Generally, one expects an increase in growth per cycle due to parasitic chemical vapor deposition (CVD) reactions when there is residual H_2O during $Al(CH_3)_3$ dosing. Yet, it is also possible that some $Al(CH_3)_3$ is consumed by parasitic CVD, at spots within the reactor that are more difficult to purge. In the remainder of this work a typical H_2O dosing time of 240 ms was used in the thermal ALD process of Al_2O_3. Under this condition, the GPC appears to be saturated while it also prevents the need for the very long purge times required when using longer H_2O dosing times.

Figure 4 shows the GPC of the remote plasma ALD process measured as a function of substrate temperature between 25 and 300°C. Data are also given for thermal ALD for substrate temperatures of 100, 200, and 300°C. For remote plasma ALD, the GPC decreases monotonically with increasing substrate temperature from

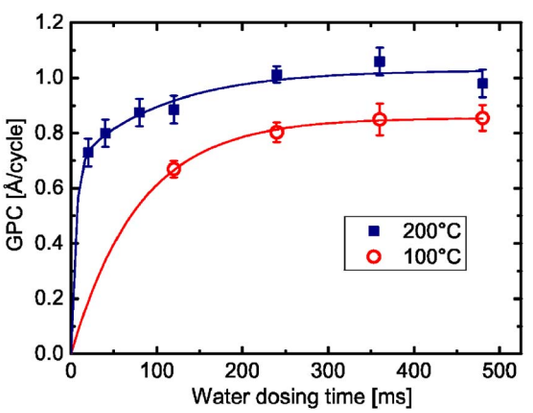

Figure 3. (Color online) GPC of thermal ALD Al_2O_3 as a function of water dosing time. Data is given for substrate temperatures of 100 and 200°C. The lines serve as a guide to the eye.

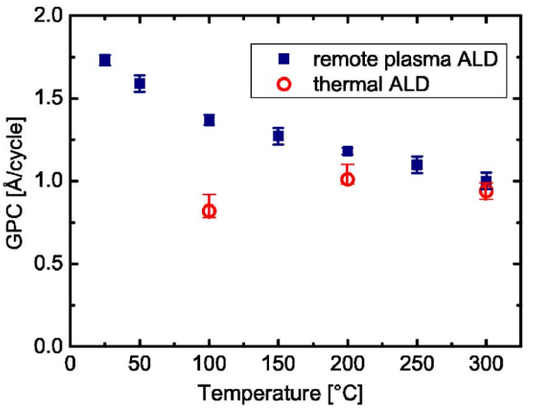

Figure 4. (Color online) GPC of Al_2O_3 as a function of substrate temperature for remote plasma and thermal ALD.

1.7 Å/cycle at 25°C to 1.0 Å/cycle at 300°C. This agrees well with values obtained in our home-built remote plasma reactor as reported previously.[8] Studies using direct plasma ALD report GPCs that are slightly higher than reported here, i.e., 1.75 Å/cycle at 100°C down to 1.0 Å/cycle at 350°C.[15,16] Remarkably, the GPC values reported for radical assisted ALD of Al_2O_3 were as high as 3.2 Å/cycle.[17] For thermal ALD the GPC is 1.0 and 0.9 Å/cycle for 200 and 300°C, respectively, which corresponds well to the literature values within the error margins.[12,16,27-29] For temperatures lower than 200°C, there is some scatter in the literature values and our GPC of 0.8 Å/cycle at 100°C is for example relatively low compared to the maximum value of 1.3 Å/cycle reported by Groner et al.[26] Although not apparent from Fig. 3, we found that it was difficult to reach saturation for the H_2O dose at 100°C. This difficulty might explain relatively low GPC at 100°C found in this study and might also explain the relatively wide spread in the literature values.

The decrease of the GPC of Al_2O_3, at increasing substrate temperature for remote plasma and thermal ALD (for substrate temperatures >200°C) is in line with observations reported in the literature for thermal ALD[12,16,27-29] and plasma assisted ALD.[15-17] This decrease is generally attributed to thermally activated recombination reactions of surface hydroxyl groups (–OH), the so-called dehydroxylation.[12,30] Assuming that the reactive Al_2O_3 surface sites created during O_2 plasma exposure are also hydroxyl groups,[18] these dehydroxylation reactions can also explain the decrease of the GPC for the remote plasma ALD case. Furthermore, note that the GPC for the remote plasma ALD process exceeded in all cases the GPC for thermal ALD. Especially at lower temperatures, this effect becomes very apparent. A similar result was reported by Lim et al.,[16] who compared direct plasma ALD with thermal ALD of Al_2O_3. It appears that the O_2 plasma is more effective as oxidant than H_2O, especially at low substrate temperatures. At higher temperatures the discrepancy becomes relatively small. This suggests that the GPC becomes dictated by the stability of the hydroxyl groups at the surface at these temperatures.

Film composition.— Figure 5 shows the RBS and ERD results for the remote plasma and thermal ALD films. The mass density, depicted in Fig. 5a was calculated from the atomic areal densities and the film thickness determined by SE. The mass density for remote plasma ALD increases from 2.6 ± 0.1 g cm^{-3} at 25°C to 3.0 ± 0.1 g cm^{-3} for temperatures higher than 200°C. The densities obtained with thermal ALD were comparable but always slightly lower than the remote plasma ALD values. Figure 5b shows that the ratio of oxygen to aluminum [O]/[Al] in the Al_2O_3 films were very similar for the remote plasma ALD and thermal ALD process. Films deposited at temperatures of 200°C and higher were stoichiometric ([O]/[Al] = 1.5) whereas the films were oxy-

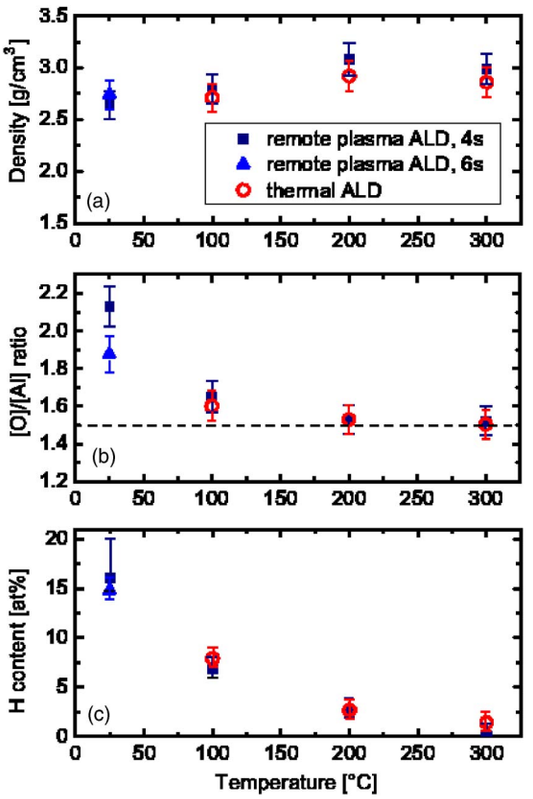

Figure 5. (Color online) Material composition as a function of substrate temperature. (a) Mass density as determined from RBS and ellipsometry. (b) [O]/[Al] ratio as determined from RBS. (c) H content as determined by elastic recoil detection. For the deposition at 25°C, data is given for both the standard recipe (4 s cycle time, 2 s plasma exposure) and for extended plasma exposure (6 s cycle time, 4 s plasma exposure).

gen rich at lower temperatures. At 25°C the [O]/[Al] ratio was even ~2.15. Figure 5c shows that the H-content in the film also increased at lower substrate temperatures. At 300°C the H-content was <1 atom % while a value over 15 atom % was reached at 25°C. Although within the absolute accuracy of the data, from a relative comparison it can be concluded that the H-content was slightly higher in the thermal ALD Al_2O_3 films. This observation is consistent with the slightly lower mass density of these films. The fact that the films increase in O and H-content at low temperatures suggests that a significant amount of hydroxyl groups are incorporated into the film at these temperatures. This is observed by the –OH stretch vibrations observed by infrared transmission spectroscopy in films deposited at 25°C.[30] The C-content was below the RBS detection limit of ~1 atom % in all cases, with the exception of the film deposited by remote plasma ALD at 25°C which contained 5 atom % carbon. Upon doubling the plasma exposure time from 2 to 4 s for this temperature, the C-content decreased below the detection limit and the film became more stoichiometric (i.e., [O]/[Al] = 1.88) and slightly denser (i.e., 2.7 ± 0.1 g cm^{-3}), as also shown in Fig. 5.

The results reported here show good agreement with the properties of the Al_2O_3 films obtained in our home-built remote plasma ALD reactor under saturated conditions.[8] Compositional data on radical-enhanced ALD yielded also similar trends but the films were more oxygen rich ([O]/[Al] = 1.81 at 100°C) and contained also more carbon, (2.3 atom % at 100°C).[17] Other studies on plasma assisted ALD of Al_2O_3 did not focus on film composition. For thermal ALD, the densities of the Al_2O_3 films agree with values obtained by Groner et al.,[26] however the H content found in the present study is somewhat lower (7.9 atom % instead of 14 atom % at 100°C). Furthermore, the refractive index of 1.64 ± 0.02 that we found for films deposited at temperatures higher than 100°C by spectroscopic elipsometry agrees well with other thermal ALD studies.[27,28] From the aforementioned results, it can be concluded that the remote plasma process yields higher growth per cycle values at reduced cycle times than thermal ALD. The material properties of remote plasma are very similar and at least as good as that of thermal ALD for substrate temperatures beyond 100°C. For low substrate temperatures, the discrepancy between remote plasma ALD and thermal ALD becomes more apparent. At low temperatures, remote plasma ALD provides the option to deposit Al_2O_3 with fair to good material properties at high growth rates, i.e., with a high growth per cycle and short cycle times.

Conformality and electrical properties.— For the application of the Al_2O_3 films as dielectric material in demanding three-dimensional topologies, both the electrical properties and the conformality of the films deposited in high-aspect ratio structures are important. Figure 6 shows a high-resolution SEM image of a remote plasma Al_2O_3-film deposited in 700 cycles at a substrate temperature of 200°C in a macropore structure with an aspect ratio of ~8:1. Arrays of such macropores are used for the synthesis of metal oxide semiconductor (MOS) "trench" capacitors that serve as rf decoupling capacitors integrated in silicon.[4] The thickness of the film measured with spectroscopic ellipsometry on the top surface of the wafer was 83 nm. The thicknesses measured with high-resolution SEM at the bottom and sidewall of the macropores was 80 ± 3 nm. The remote plasma is therefore able to deposit highly conformal films in these high aspect ratio structures. Recombination losses of reactive oxygen species such as O-radicals are apparently not significant under the present conditions. This can be understood from the low surface recombination coefficient of O-radicals on oxide surfaces.[31]

Preliminary results of the electrical characterization of Al_2O_3 films deposited by remote plasma ALD on planar substrates at a substrate temperature of 200°C are shown in Fig. 7. In this figure, the equivalent oxide thickness (EOT) values calculated from the

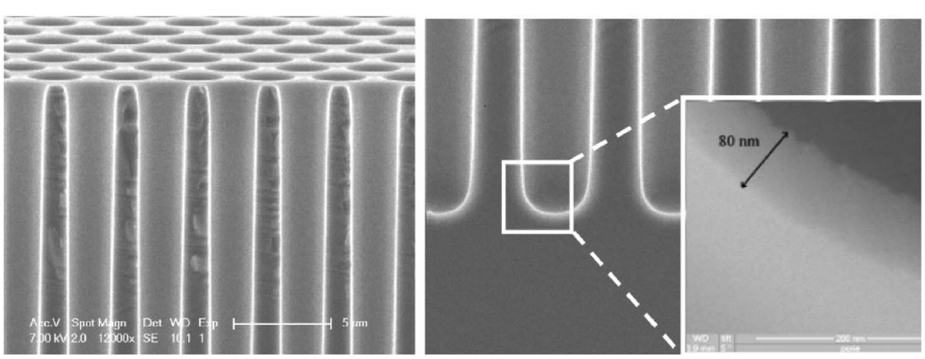

Figure 6. High-resolution SEM images of Al_2O_3 deposited by remote plasma ALD in macropore structures with an aspect ratio of ~8 (diam: 2–2.5 μm, depth: 19 μm). The Al_2O_3 was deposited using 700 ALD cycles.

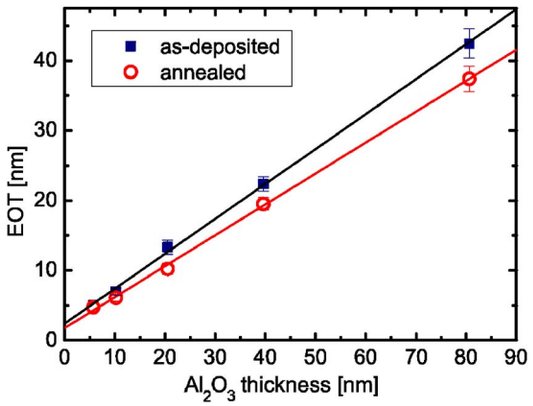

Figure 7. (Color online) EOT vs physical thickness of Al_2O_3 films deposited at 200°C by remote plasma ALD. Results for both the as-deposited and the annealed (425°C, forming gas) material are shown.

C-V measurements are shown as a function of the physical Al_2O_3 film thickness d. The EOT increases linearly with the Al_2O_3-film thickness for both the as-deposited films and for the films which were forming gas annealed at 425°C. Using the expression

$$\text{EOT} = \frac{\varepsilon_0 k(\text{SiO}_2)}{C/A} = \frac{k(\text{SiO}_2)}{k(\text{Al}_2\text{O}_3)} d(\text{Al}_2\text{O}_3) + d(\text{SiO}_2) \qquad [2]$$

where C/A is the measured capacity density and ε_0 is the vacuum permittivity, the dielectric constant can be determined as $k = 7.8$ and $k = 8.9$ for the as-deposited and annealed Al_2O_3, respectively. The offset of the linear fit can be most probably attributed to the presence of an interfacial SiO_x layer. Other ALD studies also reported on such an interfacial layer[13] and we found a 1.2 nm thick SiO_x interfacial layer for Al_2O_3 deposited in our home-built remote plasma ALD reactor.[10] Investigation of the formation of this interfacial oxide layer is outside the scope of the present study and no effort was undertaken to minimize its thickness. Furthermore, the breakdown voltage was investigated by current density measurements using the same samples. The catastrophic breakdown field, defined as the field where the current reaches the compliance setting (i.e., 100 mA) of the parameter analyzer, was determined to be 9.7 ± 0.5 MV/cm for as-deposited films and 8.4 ± 0.5 MV/cm for the postdeposition annealed films. The dielectric constants obtained here are in good agreement with those obtained in the literature for plasma ALD at 200°C.[13,16,17]Dielectric constants obtained for thermal ALD of Al_2O_3 have been summarized by Groner et al.[32] For deposition temperatures below 300°C, the dielectric constants reported were 7.6 or lower. The breakdown field reported here is relatively high but cannot easily be compared to values reported in the literature due to the use of different definitions for breakdown. Although these results are promising, more investigations are required to get full insight into the electrical properties of the Al_2O_3, also under other operating conditions.

Conclusions

The remote plasma ALD process of Al_2O_3 from $Al(CH_3)_3$ and O_2 plasma was characterized and compared to the well-established thermal ALD process of Al_2O_3 employing H_2O as the oxidant. This comparison was carried out for films deposited in the same commercial 200 mm reactor. The growth per cycle, saturation of the surface reactions, and material properties were investigated for substrate temperatures between 25 and 300°C. It was demonstrated that uniform high-quality films can be obtained for substrate temperatures above 100°C. For these temperatures, the mass densities of the remote plasma ALD films are slightly higher than those of the thermally deposited films. Remote plasma ALD also yields fair material properties below 100°C at a relatively high growth per cycle and short cycle times. Conformal films in high-aspect ratio structures were achieved using remote plasma ALD and preliminary results on electrical characterization reveal that the Al_2O_3 show good dielectric performance.

Acknowledgments

The authors thank G. Nieuwland and T. Dao of Philips Research for the high-resolution SEM and RBS measurements, respectively. The skillful technical assistance of J.J.A. Zeebregts and M.J.F. van de Sande is acknowledged. This work has been supported by the Dutch Technology Foundation STW and by SenterNovem, an agency of the Netherlands Ministry of Economic Affairs ("Innovia" project IS 044041). The research of W.M.M.K. was made possible by a fellowship from the Royal Netherlands Academy of Arts and Sciences.

Eindhoven University of Technology assisted in meeting the publication costs of this article.

References

1. E. P. Gusev, E. Cartier, D. A. Buchanan, M. Gribelyuk, M. Copel, H. Okorn-Schmidt, and C. D'Emic, *Microelectron. Eng.*, **59**, 341 (2001).
2. J. W. Lim, S. J. Yun, Y. H. Kim, C. Y. Sohn, and J. H. Lee, *Electrochem. Solid-State Lett.*, **7**, G185 (2004).
3. E. Gerritsen, N. Emonet, C. Caillat, N. Jourdan, M. Piazza, D. Fraboulet, B. Boeck, A. Berthelot, S. Smith, and P. Mazoyer, *Solid-State Electron.*, **49**, 1767 (2005).
4. F. Roozeboom, A. L. A. M. Kemmeren, J. F. C. Verhoeven, F. C. van den Heuvel, J. H. Klootwijk, H. Kretschman, T. Fric, E. C. E. van Grunsven, S. Bardy, C. Bunel, D. Chevrie, F. LeCornec, S. Ledain, F. Murray, and P. Philippe, *Thin Solid Films*, **504**, 391 (2006).
5. J. H. Klootwijk, A. L. A. M. Kemmeren, R. A. M. Wolters, F. Roozeboom, J. F. C. Verhoeven, and F. C. van den Heuvel in *Defects in High k Gate Dielectric Stacks'*, E. Gusev, Editor, p. 17, Springer, Dordrecht (2005).
6. A. Bajolet, J.-C. Giraudin, C. Rossato, L. Pinzelli, S. Bruyère, S. Crémer, T. Jagueneau, P. Delpech, L. Montès, and G. Ghibaudo, in *Proceedings of ESSDERC*, p. 121 (2005).
7. S. J. Yun, Y. W. Ko, and J. W. Lim, *Appl. Phys. Lett.*, **85**, 4896 (2004).
8. E. Langereis, M. Creatore, S. B. S. Heil, M. C. M. van de Sanden, and W. M. M. Kessels, *Appl. Phys. Lett.*, **89**, 081915 (2006).
9. P. F. Carcia, R. S. McLean, M. H. Reilly, M. D. Groner, and S. M. George, *Appl. Phys. Lett.*, **89**, 031915 (2006).
10. B. Hoex, S. B. S. Heil, E. Langereis, M. C. M. van de Sanden, and W. M. M. Kessels, *Appl. Phys. Lett.*, **89**, 042112 (2006).
11. T. M. Mayer, J. W. Elam, S. M. George, P. G. Kotula, and R. S. Goeke, *Appl. Phys. Lett.*, **82**, 2883 (2003).
12. R. L. Puurunen, *J. Appl. Phys.*, **97**, 121301-1 (2005).
13. S. C. Ha, E. Choi, S. H. Kim, and J. S. Roh, *Thin Solid Films*, **476**, 252 (2005).
14. M. Cho, H. B. Park, J. Park, S. W. Lee, C. S. Hwang, J. Jeong, H. S. Kang, and Y. W. Kim, *J. Electrochem. Soc.*, **152**, F49 (2005).
15. S. J. Yun, J. W. Lim, and J. H. Lee, *Electrochem. Solid-State Lett.*, **7**, C13 (2004).
16. J. W. Lim, and S. J. Yun, *Electrochem. Solid-State Lett.*, **7**, F45 (2004).
17. A. Niskanen, K. Arstila, M. Ritala, and M. Leskela, *J. Electrochem. Soc.*, **152**, F90 (2005).
18. S. B. S. Heil, P. Kudlacek, E. Langereis, R. Engeln, M. C. M. van de Sanden, and W. M. M. Kessels, *Appl. Phys. Lett.*, **89**, 131505 (2006).
19. J. Kim, K. Chakrabarti, J. Lee, K. Y. Oh, and C. Lee, *Mater. Chem. Phys.*, **78**, 733 (2003).
20. W. M. M. Kessels, S. B. S. Heil, E. Langereis, J. L. van Hemmen, H. C. M. Knoops, W. Keuning, and M. C. M. van de Sanden, *ECS. Trans.*, **3** (2006).
21. S. W. Choi, C. M. Jang, D. Y. Kim, J. S. Ha, H. S. Park, W. Koh, and C. S. Lee, *J. Korean Phys. Soc.*, **42**, S975 (2003).
22. J. Kim, S. Kim, H. Jeon, M. H. Cho, K. B. Chung, and C. Bae, *Appl. Phys. Lett.*, **87**, 053108 (2005).
23. S. B. S. Heil, J. L. Hemmen, M. C. M. van de Sanden, W. M. M. Kessels, C. J. Hodson, N. Singh, J. H. Klootwijk, and F. Roozeboom, Unpublished results.
24. S. B. S. Heil, E. Langereis, A. Kemmeren, F. Roozeboom, M. C. M. van de Sanden, and W. M. M. Kessels, *J. Vac. Sci. Technol. A*, **23**, L5 (2005).
25. E. Langereis, S. B. S. Heil, M. C. M. van de Sanden, and W. M. M. Kessels, *J. Appl. Phys.*, **100**, 023534 (2006).
26. M. D. Groner, F. H. Fabreguette, J. W. Elam, and S. M. George, *Chem. Mater.*, **16**, 639 (2004).
27. R. Matero, A. Rahtu, M. Ritala, M. Leskela, and T. Sajavaara, *Thin Solid Films*, **368**, 1 (2000).
28. W. Ott, J. W. Klaus, J. M. Johnson, and S. M. George, *Thin Solid Films*, **292**, 135 (1997).
29. S. D. Elliott, G. Scarel, C. Wiemer, M. Fanciulli, and G. Pavia, *Chem. Mater.*, **18**, 3764 (2006).
30. C. Dillon, A. W. Ott, J. D. Way, and S. M. George, *Surf. Sci.*, **322**, 230 (1995).
31. J. T. Gudmundsson, T. Kimura, and M. A. Lieberman, *Plasma Sources Sci. Technol.*, **8**, 22 (1999).
32. M. D. Groner, J. W. Elam, F. H. Fabreguette, and S. M. George, *Thin Solid Films*, **413**, 186 (2002).